© Universiti Tun Hussein Onn Malaysia Publisher's Office

IJIE

Journal homepage: http://penerbit.uthm.edu.my/ojs/index.php/ijie
ISSN : 2229-838X e-ISSN : 2600-7916

The International Journal of Integrated Engineering

Electrochemical Performance of $SrWO_4$ Electrolyte for SOFC

Ahmed Afif[1]*, Nikdalila Radenahmad[1], Juliana Zaini[1], Abdalla Mohamed Abdalla[1], Seikh Mohammad Habibur Rahman[1], Quentin Hoon Nam Cheok[1], Abul Kalam Azad[1]

[1]Faculty of Integrated Technologies,
Universiti Brunei Darussalam, Jalan Tunku Link, Gadong BE 1410, Brunei Darussalam

*Corresponding author

DOI: https://doi.org/10.30880/ijie.2021.13.07.009
Received 21 October 2020; Accepted 23 March 2021; Available online 30 September 2021

Abstract: Scheelite structured $SrWO_4$ material was synthesized by the solid-state sintering method and studied with respect to phase stability and ionic conductivity under condition of technological relevance for SOFC applications. The resulting compound was crystallized in the single phase of tetragonal scheelite structure with the space group of $I4_1/a$. Room temperature X-ray diffraction and subsequent Rietveld analysis confirms its symmetry, space group and structural parameters. Analysis by SEM illustrated a highly dense structure. $SrWO_4$ sample shows lower conductivity compared to the traditional BCZY perovskite structured materials. $SrWO_4$ sample exhibited an ionic conductivity of 1.93×10^{-6} S cm^{-1} at 1000℃ in dry Ar condition. Since this scheelite type compound demonstrated significant conductivity and a dense microstructure, it could serve in SOFC as a mixed ion-conducting electrolyte.

Keywords: Scheelite structure, electrolyte, SOFC, impedance

1. Introduction

SOFC has become a great blessing in recent renewable and sustainable energy sector due to its high efficiency, fuel flexibility and low pollutant emissions [1–4]. Oxygen ion-conduction requires high activation temperatures and proton-conducting materials can be thermally activated at lower temperatures than oxygen ion-conducting ones [5]. At intermediate temperatures (IT, 400-700℃), with a low activation energy and higher efficiency, a majority of perovskite-type oxides have shown high proton conductivity in H_2O and H_2 containing atmospheres [6–8]. The IT-SOFC has become cost effective system over conventional high temperature solid oxide fuel cells (HT-SOFC), as it can be manufactured more economically using less expensive stack interconnect materials [9,10]. In general, high-temperature proton conductors have been found to be oxides with oxygen deficiency in the form of oxygen vacancies, where protons dissolve as hydroxide defects in the oxide at the expense of the vacancies.

Getting the best proton-conducting electrolyte material with high chemical stability is a great challenge. The synthesis of a highly-dense ceramic proton-conducting electrolyte material at low sintering temperature is another major challenge as well. Acceptor-doped perovskites are examples of oxides containing both oxygen vacancies and protons. Some of the Ba- and Sr-containing perovskites exhibit state-of-the-art proton conductivity of about 0.01 Scm^{-1} (e.g. $BaCe_{0.9}Y_{0.1}O_{3-\delta}$) [11–14]. Meanwhile, $BaCeO_3$-and $BaZrO_3$-based materials exhibit high conductivity and good chemical stability [7,15,16]. $BaCe_{0.7}Zr_{0.25-x}Y_xZn_{0.05}O_3$ proton-conducting electrolyte was reported to be a high density and highly-conductive electrolyte in the intermediate temperature range [8,17].

Recently, alternative proton-conducting materials like acceptor-doped rare-earth materials, MTO_4, where M = La, Ca, Sr, Ba,Y, Nd, Gd, Tb, Er, Pb, Cd and T = Nb, W, Mo, Mn have been suggested to offer high CO_2 tolerances based on the scheelite structure [18–22]. Proton conductivity dominates under wet conditions up to temperatures around 1,000℃ with a contribution of p-type electronic conduction, which is significant under oxidizing conditions above 800℃.

*Corresponding author: ahmedafif03@gmail.com

$LaNbO_4$-based materials exhibit moderate conductivity while being almost pure proton conductors, and are known for their stability in CO_2-containing atmosphere and water vapor environment [18,23]. The highest proton conductivity recorded so far is for $LaNbO_4$ when it contains minor A-site acceptor substitutions, such as $Ca_{0.01}La_{0.99}NbO_{4-d}$ at 800℃ [24]. Among the scheelite crystals, $BaWO_4$ is the most efficient crystal for the development of Raman lasers [25]. The structural calculations also show $BaWO_4$ to be a direct band gap crystal, having less dispersive valence and conduction bands in contrast to other Scheelites crystals. These scheelite-type oxides exhibit a high oxide ion conduction, e.g. $Pb_{0.9}Sm_{0.1}WO_{4+\delta}$ shows a conductivity of $\sim 2\times10^{-2}$ Scm^{-1} at 800℃, which is comparable to that of YSZ (3.6×10^{-2} Scm^{-1} at 800℃) [26,27].

Though $SrWO_4$ materials originally used as photoluminescence medium, lasers hots, optical fibers, photocatalyst and antibacterial materials, this material can be used in fuel cell application. To date, except for the Czochralski technique and pulsed laser deposition, wet-chemistry routes including precipitation, polymeric precursor, solvothermal, microwave radiation and microemulsion-mediated method have been reported to prepare SrWO4 crystals [28,29]. Moreover, SrWO4 crystals allow the introduction of different lanthanide ions, which can be used as matrices for laser active elements with non-linear self conversion of radiation to a new spectral range. SrWO4 sample compound was chosen as electrolyte because Sr is highly chemically reactive and stable element. SrWO4 material has very high chance to get high ionic conductivity.

In the current study, $SrWO_4$ as scheelite material was composited to get enough highly dense electrolyte material to be used in SOFC. High density coupling with high conductivity will make this material very useful for SOFCs applications. The newly mixed ion-conducting scheelite $SrWO_4$ is abbreviated as SWO. The sample compound was synthesized by solid state reaction route (SSR) and characterized by X-ray diffraction (XRD), scanning electron microscopy (SEM), Fourier transform infrared (FTIR) and Electrochemical impedance spectroscopy (EIS).

2. Experimental

To prepare the $SrWO_4$ ceramic compound, the solid state reaction method was used. Stoichiometric amounts of $SrCO_3$ (98% purity, Aldrich, China) and WO_3 (99% purity, Aldrich, USA) were mixed with ethanol using a mortar and pestle. The finely-ground powder was first dried and subsequently calcined at 700℃ for 10 h using a heating rate of 2°C min^{-1}. A hydraulic press was utilized to make 13 mm diameter pellets under 5 tons of pressure and sintered at 900℃ in air for 10 h, each with 2℃ min^{-1} as heating and 5℃ min^{-1} cooling rate. The final sintering temperature was 1000°C in air for 10 h. The phase characterization was examined by X-ray powder diffraction using Bruker axs-D8 advance diffractometer ($CuK\alpha_1$, λ = 1.5406 Å) in the 2θ range from 10º to 90º. The data was collected with a count time of 60 sec/step and a 0.01º step size. The FullProf (ABC publishers) software was used to refine the obtained data by the Rietveld method [30]. The morphological characteristic of the prepared electrolyte was examined using FEG-SEM (JSM-7610F). The SEM morphological data was collected in an atmospherically-isolated chamber. The FTIR spectra was recorded by PerkinElmer Spectrometer for diffuse infrared spectroscopy in air at room temperature. Powder samples were standardized using a run with optically-transparent KBr, as a reference.

The electrochemical properties were examined using EIS. A Solartron 1260 frequency response analyzer was connected to a ProboStat (NorECs, Norway) system to measure impedance in a frequency range from 6 MHz to 1 mHz and the applied sine wave amplitude was 1 V rms. The sintered pelles of the as-prepared material (13 mm diameter and 0.5 cm^2 platinum pasted electrodes) were used for the impedance measurements. Impedance data was collected during the cooling cycle from 1000 to 150℃ in steps of 50℃ under a dry Ar atmosphere which was dried by passing Ar gas through two beds of P_2O_5 desiccant before entering the conductivity cell. At each temperature, enough time was allocated to ensure stability before impedance spectra was recorded. The impedance refinement program Z-View (Scribner Associates Inc.) was used to fit the experimental impedance data. The brick-layer model was employed to represent the electrical response of the samples. Each arc from the experimental data represented a parallel combination of a resistance (R) and a constant-phase element (CPE). The resistance could not be extracted reliably because of the high impedance at low temperatures, e.g. $T \leq 200$℃. No correction for sample porosity was applied to the conductivity data.

3. Results and Discussions

3.1 Phase Analysis

Figure 1 (a) shows the refinement of X-ray diffraction (XRD) patterns of all SWO compound sintered at 1000℃. In this composition, Strontium (Sr) was the A-site component and Tungsten (W) was the B-site component. XRD was carried out on the prepared samples. The patterns can be indexed as single phase scheelite type tetragonal symmetry in the $I4_1/a$ space group. There are no additional or intermediate phases were detected in SWO, which confirm the previous studies [28,29,31]. Due to behavior of Strontium as the highly chemically reactive and naturally stable element and Tungsten as heaviest and stable element, there is no changes of phases in SWO. Table 1 shows the unit cell parameters, bulk and theoretical densities and Refinement factors. Figure 1 (b) shows the schematic 3D polyhedral diagram of the tetragonal structure using VESTA software.

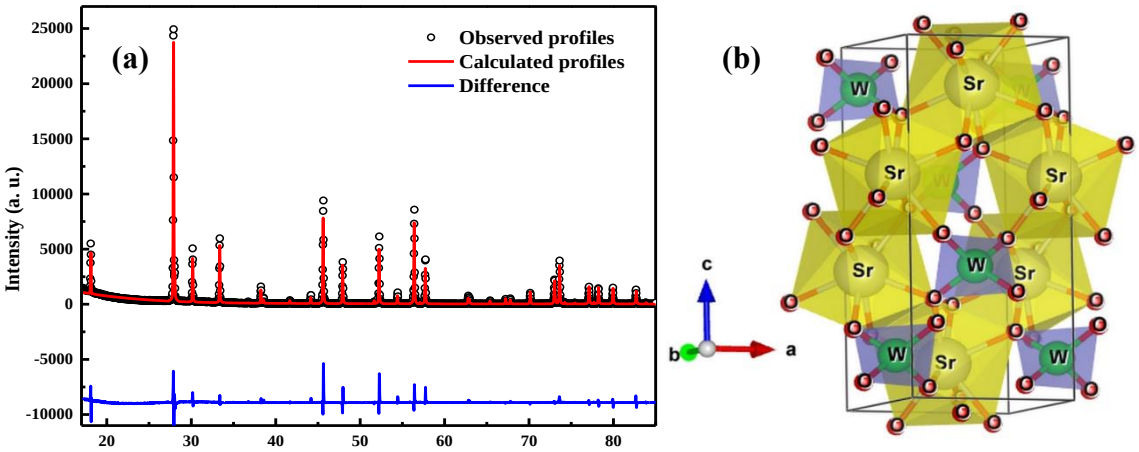

Fig. 1 - (a) Rietveld refinement profile; (b) schematic 3D polyhedral diagram of SWO in a unit cell

The figure 1 (b) also represents scheelite type structure. In the scheelite-type ABO_4 Structure, each octahedral A cation (Sr) is coordinated with eight oxygen atoms and each tetrahedral B cation (W) is coordinated to four oxygen atoms, which are common binary oxides in both natural and synthetic systems. There is no possibility for the vacancies in the anionic or cationic subdomains. The presence of Sr vacancies in the structures and the ordering of A cations and vacancies can furnish a new means for modifying their properties. Cation deficient in the compound can be considered as good ionic conductors. Thus the presence of a small percentage of dopants leads to an increased conductivity [32].

Table 1 - Rietveld refinement analysis of X-ray diffraction data for $SrWO_4$

Sample Parameters		SWO
Space group		I 4_1/a
Chi^2 (χ^2)		13.6
Cell parameter (Å)	$a = b$	5.361(1)
	c	11.828(4)
Density		6.328
Vol (Å)		340.071
No. of fitted parameter		20
R_f - factor		7.19
R_p		16.6
R_{wp}		21.2

3.2 Morphology Analysis

To observe the microstructure morphology of the SWO electrolyte, SEM analysis was carried out. Figure 2(a) shows the surface microstructure of SWO electrolyte. The surface of the sample was free of cracks. The grains were completely compacted next to each other, of a large size and well-developed. No traces of liquid or secondary phases were found at the grain boundary region in the investigated sample. This suggests that the electrolyte material has a high-density and is non-porous. The grain sizes are 1-10 µm for all compositions. The large grain size offers lower grain boundary resistance, which is beneficial for ion conduction. Figure 2(b) represents the pattern of compositions by X-ray analysis. Each chemical element has a unique electron movement that can be interpreted as energy. The figure 2 (b) can be used to describe the intensity of all SWO elements. Carbon peaks are also present because of the carbon coating on the sample's surface. The elemental composition of the compound is shown in Table 2. The results from EDX are reasonably comparable to formula values, because X-ray can be effectively used to direct the elements of compounds accurately. The use of X-ray in XRD and EDX analysis is to identify the elements of the compound.

3.3 Bonding Analysis

The FT-IR spectra of SWO compound was measured in the wave number region of 4000 cm^{-1} to 500 cm^{-1} with a resolution of 2 cm^{-1}. Figure 3 (a) presents the FT-IR spectra of SWO sample. The characteristic strong and broad absorption bands have two vibration peaks at 938 cm^{-1} to 778 cm^{-1} were assigned to O-W-O anti-symmetry stretching vibrations in the $[WO_4]$ tetrahedron. The sharp absorption peaks appeared due to symmetric bending vibrations in the $[WO_4]$ tetrahedron. Adsorbed water molecules on the surface of the sample at 1715 cm^{-1} was also detected. The photo

catalytic activity and proton conductivity were closely related to the number of -OH groups, which present on the surface of catalyst. Because the photo-generated holes (h^*) react with water and generate $\cdot$OH radicals, which can oxidize the organic pollutants. Therefore, an increase in the number of surface -OH groups could improve the proton conductivity. After hydration, the XRD was carried out to check the phase stability. Figure 3(b) shows the XRD curves of SBW1 before and after hydration process. There was no phase change during hydration.

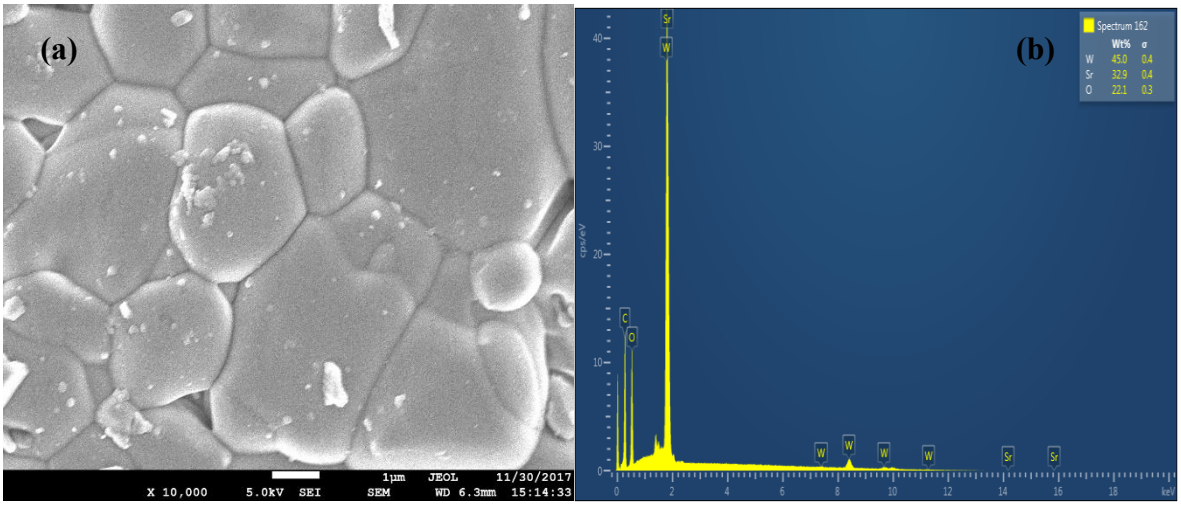

Fig. 2 - (a) SEM morphology; (b) EDX spectra of SWO

Table 2 - Compositional distribution of $SrWO_4$, where %F is composition from compound formula and %EDX is composition from EDX

Samples	Elements		Sr	W	O
SBW1	% F		16.67	16.67	66.67
	% EDX	% atomic	18.73	12.23	69.04
		% Wt	32.86	45.03	22.11

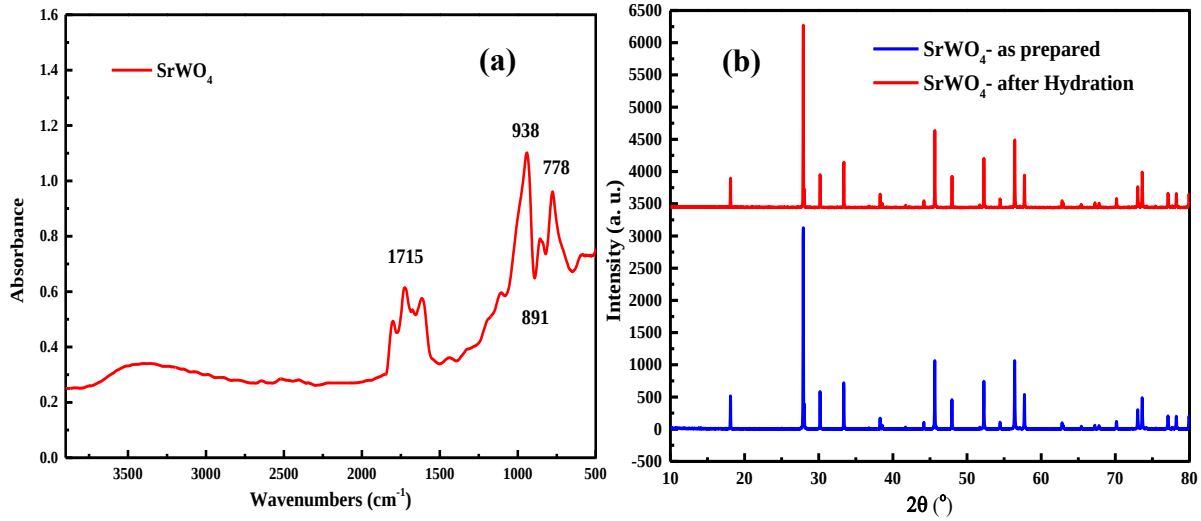

Fig. 3 - (a) FTIR of SWO; (b) Comparison of XRD after hydration test

3.4 Ionic Conductivity

The ionic conduction (as part of the electrochemical properties) of the SWO sample was investigated using AC impedance spectroscopy. Figure 4(b) shows impedance spectrum of SWO recorded at 1000 – 800℃ under dry Ar conditions with bulk and grain boundary (GB) response. A circuit model was used to estimate the GB and bulk resistance of the sample compositions. The electrode interface response was excluded from the fitting and the total resistance was calculated from the sum of the GB and bulk resistance. The presence of GB resistance in the prepared samples is indicated by the observation of more than one semicircle around 700°C under dry Ar condition. From 700°C to 1000°C, the bulk is resolved from the intercept at higher frequency intercept with real axis. The observed total frequency range was 0.1 Hz

to 6 MHz at temperature range of 700°C to 1000°C. As example, at 1000°C the frequency range was 1 KHz to 6 MHz. Above 700°C, it was difficult to separate the bulk from the grain boundary conductivities although typically 2 RC (resistance in combination with parallel to CPE) equivalent circuits in series (see figure 4(b) inset) is used.

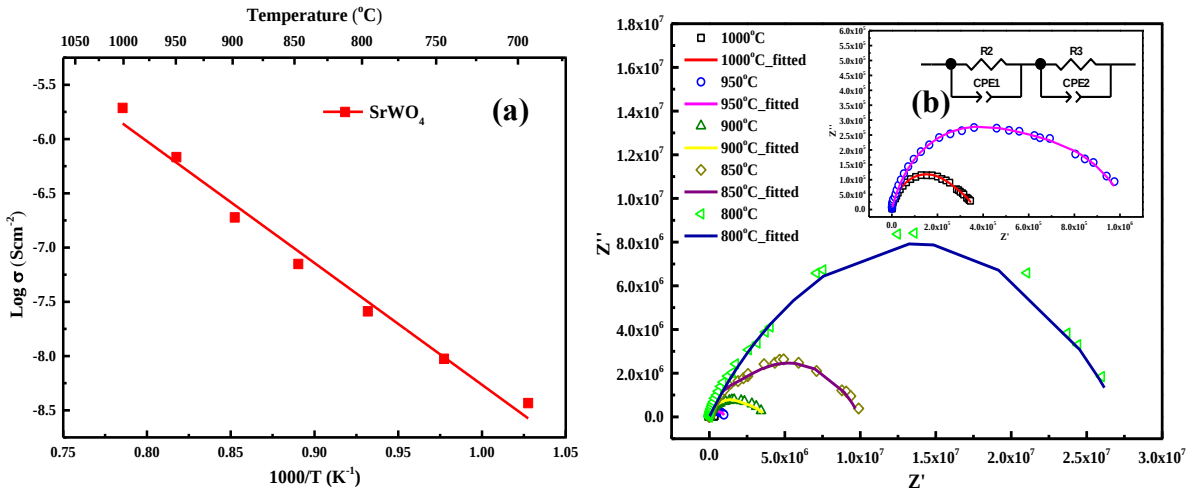

Fig. 4 - (a) Arrhenius plot of SWO; (b) Impedance spectra of SWO at 800 to 1000°C under dry Ar

Figure 4(a) shows the Arrhenius plot of SWO sample in dry Ar atmosphere. The total conductivity was 3.68×10^{-9}, 2.58×10^{-8}, 1.89×10^{-7} and 1.98×10^{-6} Scm^{-1} at 700, 800, 900 and 1000°C respectively for SWO under dry Ar atmosphere. Activation energies (Ea) for the total conductivity in dry Ar conditions was 2.2 eV. We also observed a substantially better fit with the addition of inductance, especially at higher temperature ranges (above 1000°C). The actual capacitance can be calculated using the expression given by Afif et al and Azad et al. [33,34]. The capacitance observed with the high frequency part semicircle was in the range of 10^{-12} -10^{-8} F and that of intermediate frequency range was 10^{-8}-10^{-6} F corresponding to bulk/grain-boundary and sample/electrode response, respectively [34,35]. The values of the chi-square from the equivalent circuit model fit of EIS were $4.51\times10^{+12}$, $3.62\times10^{+11}$, $2.12\times10^{+11}$, $1.17\times10^{+10}$, $2.85\times10^{+09}$, $3.34\times10^{+07}$ and $4.84\times10^{+06}$ for the temperature range of 700°C to 1000°C respectively.

4. Conclusion

In this research study, a single phase $SrWO_4$ electrolyte was synthesized via solid state reaction and the subsequent SWO electrolyte was also successfully synthesized and characterized. The Rietveld analysis of XRD data showed a tetragonal scheelite structure (S.G. $I4_1/a$). SEM morphological images showed a high density and non-porous materials which is important for electrolyte application. In terms of conductivity, the compound shows low ionic conductivity. SWO exhibited an ionic conductivity of 1.98×10^{-6} S cm^{-1} at 1000°C under dry argon conditions. From the obtained results, it indicates that these kinds of materials have a very good microstructure and significant conductivity with good stability which can be applied as electrolyte materials for SOFCs.

Acknowledgement

The authors, AA would like to thank Universiti Brunei Darussalam for providing UGS scholarship to perform this research. We are grateful to Professor Sten Eriksson to arrange the 3 months summer fellowship at the Department of Chemistry and Chemical Engineering, Chalmers University of Technology to perform this research. We are also grateful to Md Aminul Islam, Department of Geological Science, Faculty of Science (FOS), Universiti Brunei Darussalam for his great support. This work was supported by the UBD CRG project: UBD/OVACRI/CRGWG(006)/161201.

References

[1] Radenahmad, N., Afif, A., Petra, P.I., Rahman, S.M.H., Eriksson, S.-G., & Azad, A.K., (2016). Proton-conducting electrolytes for direct methanol and direct urea fuel cells – A state-of-the-art review. Renewable and Sustainable Energy Reviews, 57, 1347–1358

[2] Jacobson, A.J., (2010). Materials for solid oxide fuel cells. Chemistry of Materials, 22(3), 660–674

[3] Sasaki, K., Watanabe, K., Shiosaki, K., Susuki, K., & Teraoka, Y., (2004). Multi-fuel capability of solid oxide fuel cells, In J. Electroceramics, , pp: 669–675

[4] Afif, A., Radenahmad, N., Cheok, Q., Shams, S., Kim, J.H., & Azad, A.K., (2016). Ammonia-fed fuel cells: a comprehensive review. Renewable and Sustainable Energy Reviews, 60, 822–835

[5] Li, J., Luo, J.L., Chuang, K.T., & Sanger, A.R., (2008). Chemical stability of Y-doped Ba(Ce,Zr)O3 perovskites

in H2S-containing H2. Electrochimica Acta, 53(10), 3701–3707
[6] Azad, A.K., & Irvine, J.T.S., (2007). Synthesis, chemical stability and proton conductivity of the perovksites Ba(Ce,Zr)1−x Scx O3−δ. Solid State Ionics, 178(7–10), 635–640
[7] Tao, S., & Irvine, J.T.S., (2006). A stable, easily sintered proton-conducting oxide electrolyte for moderate-temperature fuel cells and electrolyzers. Advanced Materials, 18(12), 1581–1584
[8] Afif, A., Radenahmad, N., Lim, C.M., Petra, M.I., Islam, M.A., Rahman, S.M.H., Eriksson, S., & Azad, A.K., (2016). Structural study and proton conductivity in BaCe0.7Zr0.25−xYxZn0.05O3 (x = 0.05, 0.1, 0.15, 0.2 & 0.25). International Journal of Hydrogen Energy, 41(27), 11823–11831
[9] Steele, B., (2000). Appraisal of Ce1−yGdyO2−y/2 electrolytes for IT-SOFC operation at 500°C. Solid State Ionics, 129(1–4), 95–110
[10] Yang, J., Ji, B., Si, J., Zhang, Q., Yin, Q., Xie, J., & Tian, C., (2016). Synthesis and properties of ceria based electrolyte for IT-SOFCs. International Journal of Hydrogen Energy, 41(36 (2016)), 15979–15984
[11] Iwahara, H., (1988). Proton Conduction in Sintered Oxides Based on BaCeO3. Journal of The Electrochemical Society, 135(2), 529
[12] Bonanos, N., Ellis, B., Knight, K.S., & Mahmood, M.N., (1989). Ionic conductivity of gadolinium-doped barium cerate perovskites. Solid State Ionics, 35(1–2), 179–188
[13] Iwahara, H., Yajima, T., Hibino, T., Ozaki, K., & Suzuki, H., (1993). Protonic conduction in calcium, strontium and barium zirconates. Solid State Ionics, 61(1–3), 65–69
[14] Radenahmad, N., Afif, A., Petra, M.I., Rahman, S.M.H., Eriksson, S., & Azad, A.K., (2016). High conductivity and high density proton conducting Ba1−xSrxCe0.5Zr0.35Y0.1Sm0.05O3−δ (x = 0.5, 0.7, 0.9, 1.0) perovskites for IT-SOFC. International Journal of Hydrogen Energy, 41(27), 11832–11841
[15] Nasani, N., Dias, P.A.N., Saraiva, J.A., & Fagg, D.P., (2013). Synthesis and conductivity of Ba(Ce,Zr,Y)O3-δ electrolytes for PCFCs by new nitrate-free combustion method. International Journal of Hydrogen Energy
[16] Barison, S., Battagliarin, M., Cavallin, T., Doubova, L., Fabrizio, M., Mortalò, C., Boldrini, S., Malavasi, L., & Gerbasi, R., (2008). High conductivity and chemical stability of BaCe1−x−yZrxYyO3−δ proton conductors prepared by a sol–gel method. Journal of Materials Chemistry, 18, 5120
[17] Babilo, P., & Haile, S.M., (2005). Enhanced sintering of yttrium-doped barium zirconate by addition of ZnO. Journal of the American Ceramic Society, 88(9), 2362–2368
[18] Canu, G., Buscaglia, V., Ferrara, C., Mustarelli, P., Gonçalves Patrício, S., Batista Rondão, A.I., Tealdi, C., & Marques, F.M.B., (2017). Oxygen transport and chemical compatibility with electrode materials in scheelite-type LaWxNb1−xO4+x/2 ceramic electrolyte. Journal of Alloys and Compounds, 697, 392–400
[19] Brandão, A.D., Antunes, I., Frade, J.R., Torre, J., Kharton, V. V., & Fagg, D.P., (2010). Enhanced low-temperature proton conduction in Sr0.02La 0.98NbO4-δ by scheelite phase retention. Chemistry of Materials, 22(24), 6673–6683
[20] Haugsrud, R., & Norby, T., (2006). Proton conduction in rare-earth ortho-niobates and ortho-tantalates. Nature Materials, 5(3), 193–196
[21] Goel, P., Gupta, M.K., Mittal, R., Rols, S., Achary, S.N., Tyagi, A.K., & Chaplot, S.L., (2015). Inelastic neutron scattering studies of phonon spectra, and simulations of pressure-induced amorphization in tungstates AWO4(A = Ba, Sr, Ca and Pb). Physical Review B, 91(9), 094304
[22] Benmakhlouf, A., Errandonea, D., Bouhemadou, A., Bentabet, A., Maabed, S., Bouchenafa, M., & Bin-Omran, S., (2017). Ab initio study of the mechanical and electronic properties of scheelite-type XWO4(X = Ca, Sr, Ba) compounds. International Journal of Modern Physics B, 31(12), 1750086
[23] Haugsrud, R., & Norby, T., (2006). High-temperature proton conductivity in acceptor-doped LaNbO4. Solid State Ionics, 177(13–14), 1129–1135
[24] Brandao, A.D., Gracio, J., Mather, G.C., Kharton, V. V, & Fagg, D.P., (2011). B-site substitutions in LaNb 1− x M x O 4− δ materials in the search for potential proton conductors (M= Ga, Ge, Si, B, Ti, Zr, P, Al). Journal of Solid State Chemistry, 184(4), 863–870
[25] Basiev, T.., Sobol, A.., Voronko, Y.., & Zverev, P.., (2000). Spontaneous Raman spectroscopy of tungstate and molybdate crystals for Raman lasers. Optical Materials, 15(3), 205–216
[26] Thangadurai, V., Knittlmayer, C., & Weppner, W., (2004). Metathetic room temperature preparation and characterization of scheelite-type ABO4 (A = Ca, Sr, Ba, Pb; B = Mo, W) powders. Materials Science and Engineering: B, 106(3), 228–233
[27] Esaka, T., (2000). Ionic conduction in substituted scheelite-type oxides. Solid State Ionics, 136–137, 1–9
[28] Li, X., Song, Z., & Qu, B., (2014). Shape-controlled electrochemical synthesis of $SrWO_4$ crystallites and their optical properties. Ceramics International, 40(1 PART A), 1205–1208
[29] Cavalcante, L.S., Sczancoski, J.C., Batista, N.C., Longo, E., Varela, J.A., & Orlandi, M.O., (2013). Growth mechanism and photocatalytic properties of SrWO4 microcrystals synthesized by injection of ions into a hot aqueous solution. Advanced Powder Technology, 24(1), 344–353
[30] Rodríguez-Carvajal, J., (1993). Recent advances in magnetic structure determination by neutron powder diffraction. Physica B: Condensed Matter, 192, 55–69

[31] Sczancoski, J.C., Cavalcante, L.S., Joya, M.R., Espinosa, J.W.M., Pizani, P.S., Varela, J.A., & Longo, E., (2009). Synthesis, growth process and photoluminescence properties of SrWO4 powders. Journal of Colloid and Interface Science, 330(1), 227–236

[32] Dirany, N., McRae, E., & Arab, M., (2017). Morphological and structural investigation of SrWO4 microcrystals in relationship with the electrical impedance properties. CrystEngComm, 19(34), 5008–5021

[33] Barsoukov, E., & Macdonald, J.R., (2005). Impedance Spectroscopy: Theory, Experiment, and Applications. John Wiley & Sons, Inc

[34] Rahman, S.M.H., Norberg, S.T., Knee, C.S., Biendicho, J.J., Hull, S., & Eriksson, S.G., (2014). Proton conductivity of hexagonal and cubic BaTi1-xScxO3-δ ($0.1 \leq x \leq 0.8$). Dalton Transactions (Cambridge, England : 2003), 43(40), 15055–64

[35] Irvine, J.T.S., Sinclair, D.C., & West, A.R., (1990). Electroceramics: characterization by impedance spectroscopy. Advanced Materials, 2(3), 132–138